真空电子束焊接热源建模及功率密度分析

罗 怡[1,2], 许惠斌[1], 李春天[1], 伍光凤[1]
(1. 重庆理工大学 材料科学与工程学院, 重庆 400050;
2. 西北工业大学 材料学院, 西安 710072)

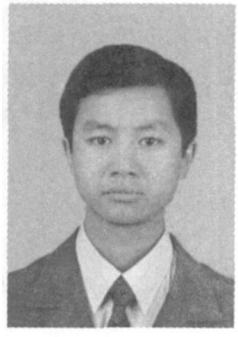
罗 怡

摘 要: 分析了真空电子束深熔焊接的热源作用形成钉状焊缝的特征, 建立了峰值功率递增型旋转高斯体热源, 即热源作用半径在深度方向呈高斯规律递减, 热源功率密度在深度方向呈指数函数规律递增. 利用该热源模型计算了聚焦状态和散焦状态下, 真空电子束焊接特殊热效应的功率密度分布. 结果表明, 热源数学模型得到的功率密度分布规律符合理想状态下的电子束热源作用特征, 可用于不同聚焦状态下的真空电子束焊接的热效应数值模拟研究.

关键词: 电子束焊接; 体热源; 功率密度
中图分类号: TG156 文献标识码: A 文章编号: 0253-360X(2010)09-0073-04

0 序 言

真空电子束焊接是一种功率密度极高的焊接方法. 在真空中, 经过聚焦的电子束流高速作用于材料表面, 形成高功率密度的焊接热源. 对于高功率焊接热源的早期研究, 多为点热源或线热源的近似考虑[1]. 多年以来, 对于电子束这种高功率密度的焊接热源的研究已经不局限于此, 并较全面地考虑了匙孔效应等高功率焊接热源焊接过程的特殊物理效应[2,3].

大量的研究结果表明, 真空电子束焊接热源为热流集中分布的体热源. 电子束热源一方面产生匙孔效应, 使电子束可以直接作用于匙孔底部的熔池壁面上, 获得深熔焊接效果[4]. 另一方面, 由于金属材料中一些合金元素沸点低, 在电子束热源作用下发生强烈的蒸发现象, 形成高温金属蒸汽等离子体, 其热效应使焊缝表面产生较大开口, 从而形成钉状焊缝. 针对电子束焊接热源的这种特殊的热效应, 建立了符合真空电子束焊接的峰值功率递增型旋转高斯体热源, 并利用该热源模型计算了不同聚焦状态下, 真空电子束焊接特殊热效应下的功率密度分布. 研究有利于分析电子束焊接热源的热效应特征和进一步对真空电子束焊接的数值模拟.

收稿日期: 2009-05-11
基金项目: 重庆市教委科学技术研究资助项目(KJ100826); 江苏科技大学先进焊接技术省级重点实验室开放研究基金资助课题

1 焊接热源功率密度计算模型

1.1 物理模型分析

常规熔化焊接过程中, 电弧热源功率密度相对较低, 电弧热作用速度较慢, 并主要以热传导的形式作用于材料; 电子束流是高功率密度的焊接热源, 电子束焊接过程中, 在高电压加速的作用下, 聚焦的电子束流高速冲击材料表面, 使表层材料瞬间熔化并蒸发. 在蒸发压力的作用下, 熔化金属被排开, 电子束流深入工件内部, 直接穿透材料, 即产生显著的匙孔效应. 在匙孔效应下的电子束焊接, 是一种焊接能量的直接作用机制, 能够实现深熔焊接的效果, 电子束流作用的物理模型如图 1所示. 匙孔中充满高温金属蒸汽, 高速电子与气态金属原子的交互作用产生的热效应、碰撞效应及光化效应, 使匙孔中的金属原子产生部分电离. 因此, 匙孔内形成包括金属中性原子、带电离子与电子在内的金属蒸汽等离子

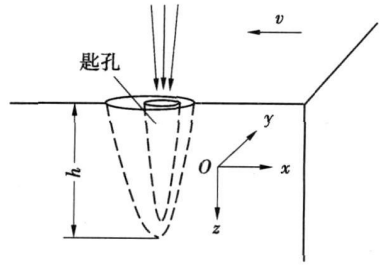

图 1 物理模型
Fig. 1 Physical model

体，并与外部焊接真空环境形成一定的压力梯度，使等离子体不断从匙孔中喷出．金属蒸汽等离子体在焊缝表面形成局部平衡，其热效应使之犹如一个特殊的高斯热源，加热焊缝表面，并使真空电子束焊缝形成较大的开口，即钉状焊缝．

由此可见，电子束焊接热源的综合热效应需要考虑高温金属蒸汽等离子体的表面高斯型热效应，同时也包括表面以下电子束流对熔池的深挖掘作用产生的热效应，随着电子束作用半径的递减，其功率密度分布沿深度方向呈有规律的递增变化．真空电子束焊接热源的这种功率密度分布规律可用图 2所示旋转高斯体模型描述．

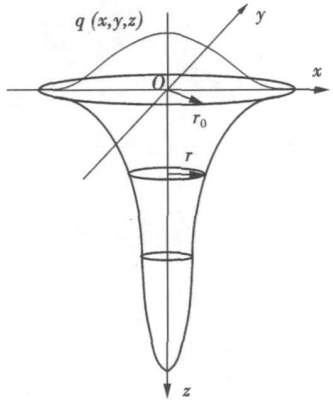

图 2 旋转高斯体模型

Fig. 2 Model of whirling Gaussian body source

1.2 热源数学模型

为了描述图 2所示的热源功率密度分布规律，建立真空电子束焊接热源功率密度递增型分布的旋转高斯体数学模型．对于旋转体热源，其功率密度分布的一般形式为

$$q(x,y,z)=q_m\exp\{-\frac{3r^2}{[R(z)]^2}\} \tag{1}$$

式中：$q(x,y,z)$为笛卡儿坐标系内任一位置处的焊接热源功率密度分布，并且根据旋转体的坐标特征可以得出 $x^2+y^2=r^2$，q_m为功率峰值，根据功率平衡方程，可以得到

$$q_m=\frac{9Q}{\pi h_0^2} \tag{2}$$

式中：Q为电子束热源有效功率，对于加速电压为 U，焊接束流为 I的电子束热源，其有效功率为

$$Q=UI\eta \tag{3}$$

式中：η为有效功率系数．

在深度方向上，热源半径呈一定变化趋势，这里将体热源的作用半径 R表示为深度 z的函数．设旋转体热源的半径在深度方向呈高斯衰减，即 $R(z)$满足高斯函数

$$R=h\exp(-\frac{3R^2}{r_0^2}) \tag{4}$$

由式（2）可得

$$R^2(z)=-\frac{r_0^2}{3}\ln(\frac{z}{h}) \tag{5}$$

式中：z的取值范围为（0，h），假设距离热源中心为 r_0的位置，电子束功率密度将为最大热流密度的 5%，h为电子束热源的有效作用深度．

随着热源的有效作用半径递减，峰值功率密度沿深度方向递增，用峰值功率密度递增函数 $I(z)$表达该递增效应，用指数函数描述这种递增规律，在式（1）中将 $I(z)$与 q_m合并考虑该递增效应，即

$$q(x,y,z)=q_mI(z)\exp\{-\frac{3r^2}{[R(z)]^2}\} \tag{6}$$

$$I(z)=\exp(\beta I_z) \tag{7}$$

式中：β为峰值功率密度递增系数，该系数的取值与聚焦电流相关，随着聚焦状态的变化，β在负值与正值之间变化．当聚焦状态为散焦的时候，β为负值，当聚焦位置为下聚焦时，β为正值；I为聚焦电流．

根据式（3），式（4），式（6），式（7）最终建立的真空电子束焊接功率密度分布的旋转高斯体模型为

$$q(x,y,z)=\frac{9Q}{\pi h_0^2}\exp(\beta I_z)\exp[\frac{9r^2}{r_0^2\ln(z/h)}] \tag{8}$$

根据该模型，可以计算真空电子束焊接过程中，采用不同的焊接参数焊缝不同位置的热源功率密度分布．

2 电子束热源功率密度分析

由于真空电子束焊接的应用要求电子束具有较大的束流密度，这就要求形成横截面压缩或收敛的电子束电子枪，这就是应用于电子束焊接的球面阴极收敛圆形电子束电子枪，它能使阴极发射的电子以锥束会聚于阳极．为了让电子束能够穿过阳极，功率较大的电子枪直接在阳极上开孔．电子束在穿过阳极孔之后便要开始发散，且阳极孔的存在也会加重电子束出阳极孔后的发散趋势．因此，电子枪引出电子束后，一般使用磁透镜聚焦方式维持电子束．在聚焦磁场或电场的作用下，可以认为阴极发射穿过阳极孔的电子具有旋转与子午面（r与 z，图 2）两个方向的运动，则在理想状态下大体形成具有圆形横截面的电子束．

图 3为通过模型计算得到的聚焦状态下，工件表面（h= 0 mm）和距离工件表面 3 mm处（h= 3 mm）的电子束焊接热源功率密度分布，其中加速电

压为 30 kV，焊接束流为 30 mA. 可见在圆形横截面电子束的作用下，功率密度类似于层层叠加的面热源. 随着电子束作用在材料上深度的增加，热源作用的区域递减，同时热源功率密度在圆形面的分布递增，在 h=0 mm处，热源功率密度峰值为 5×10^5 W/mm²，而在 h=3 mm处，热源功率密度峰值递增为 7.25×10^5 W/mm². 对于每层热源面，功率密度为不均匀对称分布，靠近热源边缘，功率密度相对较低，且在电子束热源作用区域的圆形横截面的径向，热源功率密度呈高斯规律递增. 电子束热源这样的功率密度分布，有利于熔池底部产生强烈的熔化和蒸发，从而维持匙孔效应，实现大深宽比深熔焊接.

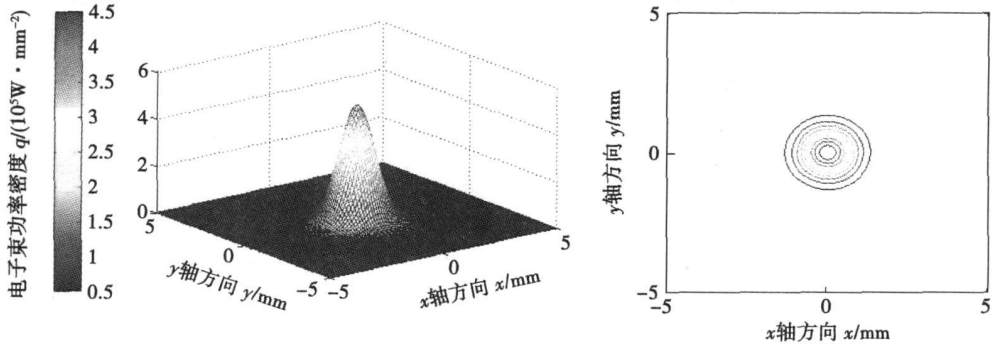

(a) 工件表面功率密度分布，h=0

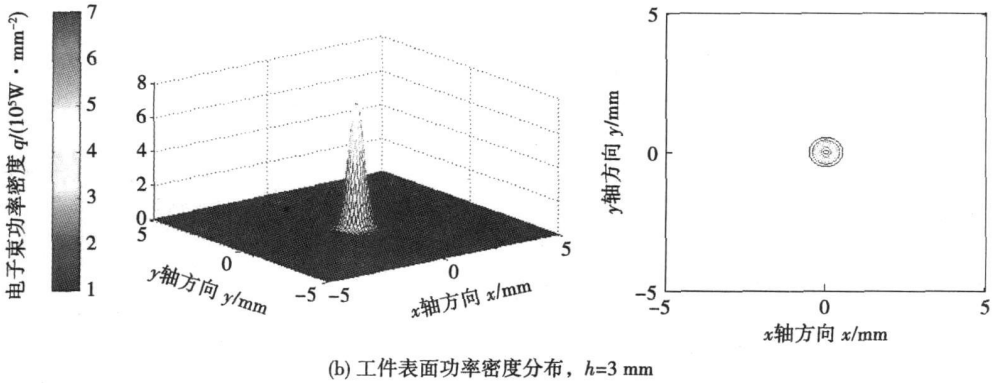

(b) 工件表面功率密度分布，h=3 mm

图 3　聚焦状态下的电子束功率密度分布

Fig. 3　Power density distribution of electron beam with focusing effect

电子束散焦状态下，由于高能量密度的电子束活性区远离工件，位于表面以上，作用于工件不同深度的热源功率密度相对较低，如图 4所示，为散焦状态时相同焊接参数下，距离工件表面 3 mm处（h=3 mm)的电子束焊接热源功率密度分布，功率密度峰值约为 3.2×10^4 W/mm²，功率密度的衰减是比较显著的，其深熔焊接的效果也会受到影响. 由于电子束作用区域的能量密度大大降低，导致熔池孔壁产

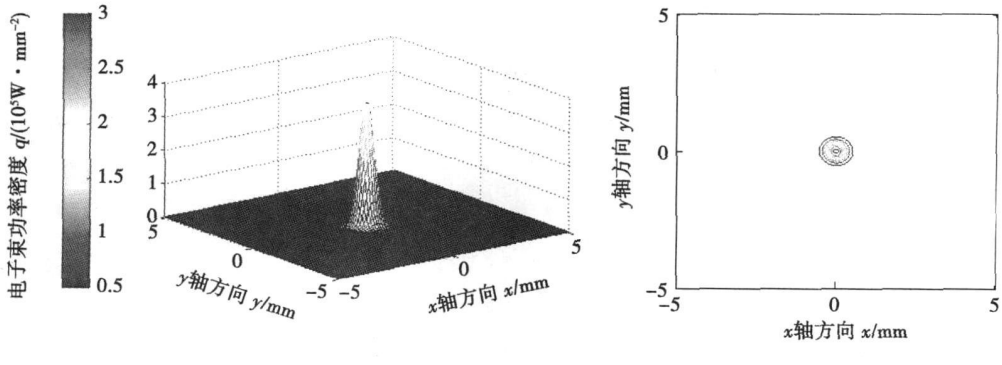

图 4　散焦状态下的电子束功率密度分布（U=60 kV，I=30 mA，h=3 mm)

Fig. 4　Power density distribution of electron beam with defocusing effect

生强烈熔化,从而无法得到大深宽比焊缝.

3 结 论

(1)建立了用于真空电子束焊接的峰值功率递增型旋转高斯体热源数学模型,在深度方向上,热源作用半径呈高斯递减,而峰值功率密度呈指数函数递增.

(2)热源数学模型得到的功率密度分布规律符合理想状态下电子束热源作用特征,可用于不同聚焦状态下的真空电子束焊接的热效应数值模拟研究.

参考文献:

[1] Rosenthal D. The theory of moving sources of heat and its application to metal treatments[J]. Transactions ASME, 1946, 43(11): 849-866.

[2] Wei P S, Ho C Y, Shian M D, et al. Three-dimensional analytical temperature field and its application to solidification characteristics in high or low-power density-beam welding[J]. International Journal of Heat and Mass Transfer, 1997, 40(10): 2283-2292.

[3] Ho C Y, Wei P S. Energy absorption in a conical cavity truncated by spherical cap subject to a focused high-intensity beam[J]. International Journal of Heat and Mass Transfer, 1997, 40(8): 1895-1905.

[4] Ho C Y, Wen M Y, Lee Y C. Analytical solution for three-dimensional model predicting temperature in the welding cavity of electron beam[J]. Vacuum, 2008, 82: 316-320.

作者简介:罗 怡,男,1979年出生,博士研究生,讲师. 主要从事焊接工艺及其设备自动化方面的教学和科研工作. 发表论文 20 余篇.

Email: luoyi@cqut.edu.cn

[上接第 72页]

bonding of titanium alloy and stainless steel[J]. Hot Working Technology, 2007, 36(3): 86-89.

[2] Zhang Huiwen, Yue Xin, Zhang Jiuhai, et al. Tendency and research status on brazing and diffusion bonding for titanium as well as its alloy to stainless steel[J]. Welding, 2006(1): 11-16.

[3] Sun Ronghu, Zhang Jiuhai. Research present situation and welding problem of titanium as well as its alloy to steel[J]. Aerospace Material Technology, 1997, 27(2): 7-11.

[4] Ohashi O. Diffusion bonding of different metal material[J]. Journal of Japan Welding Institute, 1988, 56(3): 13-17.

[5] Qin Bin, Sheng Guangmin, Yuan Jianxin, et al. Characteristic and welding method on diffusion bonding of titanium alloy and stainless steel[J]. Welding Technology, 2007, 36(3): 7-9.

[6] Qin Bin, Sheng Guangmin, Huang Jiawei, et al. Fracture analysis of diffusion bonded joint between titanium alloy and stainless steel[J]. Iron Steel Vanadium Titanium, 2005, 26(4): 55-59.

[7] Sun Ronglu, Yang Wenjie, Yu Bin, et al. Seletion of medium metal in diffusion bonding of titanium alloy and stainless steel[J]. Aerospace Material Technology, 1997, 5: 15-18.

[8] Zhang Qiufeng. Ultrasonic diffusion bonding of titanium alloy and stainless steel[J]. Mechanical Engineering and Automation, 2008, 4(11): 125-127.

[9] Wang Yanfang. Research of technology on diffusion bonding of kentanium and titanium alloy in vacuum[J]. Welding Technology, 2007, 36(5): 11-13.

[10] Osamu Taguchi, Yoshiaki Lijima, Kenichi Hirano. Reaction diffusion in the Cu-Ti system[J]. Journal of the Japan Institute of Metals, 1990, 54(6): 619-627.

作者简介:刘树英,女,1961年出生,博士,副教授. 主要从事异种材料的焊接和金属热处理. 发表论文 10余篇.

Email: Liusy168@yahoo.com.cn

tion paths layer by layer and prolonging the interfomational intervals, the cracks could be avoided.

Key words: surfacing; rapid forming; metal cored wires; cracks; segregation

Effect of loading rate on shear strength of SnAgCu solder joint LU Wei, ZHANG Ning, SHI Yaowu, LEI Yongping (School of Materials Science and Engineering, Beijing University of Technology, Beijing 100124, China). p. 57—60

Abstract: Effect of loading rate on shear strength and fracture mode of SnAgCu (SAC) lead-free solder joint was investigated. The Ag content of the solders used in the experiment was 1% to 3%. The loading rate of the solder joint was 0.01 mm/s to 10 mm/s. The results indicated that the shear strength increased with the increase of loading rate and fracture with ductile feature occured inside the solder when the loading rate was less than 1 mm/s. When loading rate reached to 10 mm/s, the shear strength decreased and brittle fracture occured in the intermetallic compounds layer of joint. Moreover, shear strength increased with Ag content of solder increased at low loading rate, while the shear strength of solder joint with 2% Ag was the lowest at high loading rate.

Key words: lead-free solder; loading rate; shear strength

Effect of vanadium on property of Fe-Cr-C hardfacing alloy WANG Zhihui, HE Dingyong, YU Changli, JIANG Jianmin (College of Materials Science and Engineering, Beijing University of Technology, Beijing 100124, China). p. 61—64

Abstract: Vanadium was added to Fe-Cr-C hardfacing alloy and its effect on the property of the alloy when welded and reheated was studied. The hardfacing layers were produced on Q235 mild steel by submerged arc welding method. The microstructures, worn surface of the overlayer were examined by means of optical microscope and scanning electron microscopy (SEM). Abrasive wear resistance and hardness were tested. The results showd that heating process had effect on the hardness of the alloy. The hardness of matrix decreased more than 22% by reheating. The max hardness decreased 37.7% with no vanadium. But it has little effect on the hardness of primary carbide of which the hardness decreased only 1.4%-11.3% by reheating. Vanadium could increase the abrasion property of post-heated Fe-Cr-C hardfacing alloy. Using the loss weight of quenched 45# sample as abrasion test bench mark, the lative abrasion value of the alloy content of 0.4% vanadium was 1.9. In the same condition, that of the alloy with no vanadium content was only 1.3. The abrasion property increased 46%.

Key words: Fe-Cr-C hardfacing alloy; vanadium element; post heat treatment; carbide; abrasion wear

Simulation of temperature field and residual stress field of thin inner layer on butt welding of clad pipe YU Jianrong, HE Xiaoxiang[2], WU Bo, CHEN Haiyang, LI Xiaodong (1. School of Mechanical Engineering, Beijing Institute of Petrochemical Technology, Beijing 102617, China; 2. College of Mechanical and Electrical Engineering, Beijing University of Chemical Technology, Beijing 100029, China). p. 65—68

Abstract: The clad pipe has a thin inner layer made of stainless steel and a thick outer layer made of carbon steel, and the outer layer has some restriction on the temperature change surrounding the inner layer when butt-welding the inner layer. With finite element method, the temperature field was computed when butt-welding inner layer and the stress field of inner layer was computed after butt welding. The convection, radiation and contact effect between the two layers were considered in the FEM model as well as temperature depended material properties. Internal heat generation loading method was applied to simulate heat source, and model change ability to simulate butt-weld. The velocity of inner layer butt-weld, the temperature and stress field of the inner layer were discussed. Meanwhile the influence of the properties of material, geometry of the plate and the welding heat input on buckling distortion were analyzed based on the simulations. The results indicate that the geometry of the plate and the welding heat input have more effect on distortion than the properties of material.

Key words: clad pipe; butt-weld; finite element analysis; stress field; contact effect

Microstructure characteristic and performance of bonding interface between titanium alloy/copper/GCr15 LIU Shuying, ZHANG Guifeng, LU Guangbao, XU Peili, WANG Yawei (1. Henan Province Key Laboratory of Advanced Non-ferrous Metals, School of Materials Science and Engineering, Henan University of Science and Technology, Luoyang 471003, Henan, China; 2. Welding Research Institute, Xi'an Jiaotong University, Xi'an 710049, China; 3. Department of Electrical and Electronic, Henan Technician College of Economics and Business, Xinxiang 453700, Henan, China; 4. Shanghai Heavy Machinery Plant Limited Corporation, Shanghai 200245, China). p. 69—72, 76

Abstract: Difficulty for diffusion bonding of different structure of titanium alloy/bearing steel restricts the application of titanium alloy. The mechanical properties of Ti-6Al-4V/Cu/GCr15 joints were evaluated by electronic tensile machine. The microstructure characteristic and performance of the bonding interface were analyzed by scanning electron microscopy and EDX. Microhardness, the fracture characteristics and area of intermetallic compounds of the joints were analyzed by X-ray diffraction. The results indicated that the tensile strength of the joints under the bonding time 1.8 ks, pressure 4.9 MPa, rises with the bonding temperature, the tensile strength of joint reaches a maximum of 206 MPa in 1 273 K. The extension bonding time caused the intermetallic compound thickness to increase which would do harm to the joints performance. α-Ti(Cu) solid solution which was generated in bonding interface was advantageous to enhance the joints performance. However, the Ti_xCu_y had more influence on joints performance which was Ti_2Cu, Ti_2Cu_3, (Ti_3Cu_4) FeTi, those caused the joint strength to go down. Copper foil should not be too thick to be as interlayer in titanium/GCr15.

Key words: interlayer; diffusion bonding; bonding interface; tensile strength; intermetallic compounds

Heat source modeling and power density analysis for vacuum electron beam welding LUO Yi[2], XU Huibin, LI Chuntian, WU Guangfeng (1. School of Material Science and Engineering, Chongqing University of Technology, Chongqing 400050, China; 2. School of Material Science and Engineering, Northwestern Polytechnical University, Xi'an 710072, China). p. 73—76

Abstract: The characteristics of heat source for vacuum electron beam welding of deep penetration were analyzed. On the basis of the gaussian descending for heat source radius and exponential increasing for power density of heat source along the depth, a mathematical model of whirling gaussian body source with increasing peak power was established. Under the level of focusing and defocusing, the power density distribution for special thermal effect of vacuum electron beam welding was calculated by this model. The results of these calculations showed that the power density distribution of the heat source model was consistent with the thermal characteristic of electron beam source based on the idealized state. And this model was applicable to the thermal effect simulation of vacuum electron beam welding at different focus levels.

Key words: electron beam welding; body source; power density

Microstructure investigation of Nd: YAG laser welded 5A90 aluminium-lithium alloys / CUI Li1, LI Xiaoyan1, HE Dingyong1, CHEN Li1, GONG Shuili2 (1. College of Materials Science and Engineering, Beijing University of Technology, Beijing 100124, China; 2. High Energy Density Beam Processing Technology Department, Beijing Aeronautical Manufacturing Technology Research Institute, Beijing 100024, China). — p77—80, 84

Abstract: Nd: YAG laser welding of 5A90 aluminium-lithium(Al-Li) alloy thin sheets has been carried out. Microhardness tests across the transverse section of the weld were performed. The influence of laser welding on the microstructure of 5A90 aluminium-lithium alloy at different sections has been evaluated by optical microscope, SEM and TEM. Microhardness tests revealed that the laser weld had lower microhardness than that of base metal. Laser welds revealed the formation and presence of a zone of equiaxed grains (EQZ) along the fusion boundary. The major strengthening phase in 5A90 aluminium-lithium alloy was δ′ phase particles. The presence of the δ′ precipitates in the welds was proved by the $L1_2$ superlattice reflections in diffraction patterns, but the volume of the δ′ precipitates in the weld zone was very little, which attributed to the decrease in the microhardness of the weld compared with the base metal.

Key words: aluminium-lithium alloys; laser welding; microstructure; δ′ precipitates

Welding TC4 thin plates by revolution pressing in welding process / ZHANG Yongxi2, YANG Jianguo1, LIU Xuesong1, FANG Hongyuan1 (1. State Key Laboratory of Advanced Welding Technology Production, Harbin Institute of Technology, Harbin 150001, China; 2. School of Material Science and Engineering, Liaoning Technical University, Fuxin 123000, Liaoning, China). — p81—84

Abstract: The welded residual compression stress which is larger than the critical compression stress will cause buckling distortion of TC4 thin plate after normal welding. In order to decrease buckling distortion, the method of revolution pressing in welding process was utilized to gain plastic extension in the high temperature zone of the welding bead. The residual stress can be reduced by compensating the plastic shrinkage in the high temperature zone. Tensile test, SEM analysis of the tensile testing specimen and measurement of the joints distortion after welding were carried out. The results showed that the deflection could be decreased to two thirds of the original deflection after the high temperature zone metal received revolution pressing. With increased pressing loading, the deflection reduced. In a word, the method of revolution pressing in welding process is feasible to control the deflection of TC4 thin plate weldment.

Key words: revolution pressing in welding process; TC4; buckling distortion; thin plat welding

Electron beam brazing repair of K465 Ni-base superalloy blades / WANG Gang1, CHEN Guoqing1, ZHANG Binggang1, FENG Jicai1, LU Chenglai2 (1. State Key Laboratory of Advanced Welding Production Technology, Harbin Institute of Technology, Harbin 150001, China; 2. AVIC Shenyang Liming Aero Engine (Group) Limited Corporation, Shenyang 110043, China). — p85—88

Abstract: The vacuum electron beam brazing (VEBB) of K465 Ni-base superalloys blades with self-made filler metal was studied. Effects of through slot (grinding off all the cracks) and non-through slot (grinding off 80% to 90% the cracks) on the cracks of joints were investigated. It's discovered very few through slot specimens have cracks and all non-through specimens have cracks. Microstructure of the brazed joints with self-made filler metal was studied by means of scanning electron microscopy (SEM), energy disperse spectrum (EDS) and X-ray diffraction (XRD). The results show that the structure of brazing seam consists of Ni-base γ solid solution, Ni_3Si, Ni_3B, Ni_3Al and Ni_3Si.

Key words: electron beam brazing; Ni-base superalloy blades; interfacial reaction product

Effect of laser power on welding process stability of Nd: YAG laser-short circuit MAG hybrid welding / WANG Wei, LIN Shangyang, WANG Xuyou, LEI Zhen (1. Harbin Welding Institute, Harbin 150080, China). — p89—92

Abstract: The effect of laser power on welding process stability and the formation of weld were investigated during Nd: YAG laser-short circuit MAG hybrid welding in this paper. The results showed that laser power was an important welding parameter which could affect welding process stability. When short-circuit MAG welding process combined with laser power, welding process would become stable. But it was not true that welding stability would rise with laser power increased. The most stable welding process presented when laser power was lower. So according to the laser power, Nd: YAG laser-short circuit MAG hybrid welding could be classified into three stages: the stabilizing arc stage with lower laser nower, transition stage and deepening weld penetration stage with higher laser power. Finally, the reasons for how laser made arc to be more stable were analyzed.

Key words: laser welding; arc welding; hybrid welding; GMAW

Effect of Al content on properties of Zn-Al filler metal / ZHANG Mao1,2, XUE Songbai1, DAI Wei1, LOU Yinbin2, WANG Shufeng3 (1. College of Materials Science and Technology, Nanjing University of Aeronautics and Astronautics, Nanjing 210016, China; 2. College of Mechanical Engineering, Huaiyin Institute of Technology, Huaian 223001, Jiangsu, China; 3. Zhejiang Xinrui Welding Material Limited Corporation, Shengzhou 312000, Zhejiang, China). — p93—96